

## 3D Gauss-Newton inversion of surface-borehole TEM data

Chong Liu<sup>a</sup>, [chong.liu@uqat.ca](mailto:chong.liu@uqat.ca)

LiZhen Cheng<sup>a</sup>, [lizhen.cheng@uqat.ca](mailto:lizhen.cheng@uqat.ca)

Michel Chouteau<sup>b</sup>, [michel.chouteau@polymtl.ca](mailto:michel.chouteau@polymtl.ca)

Fouad Erchiqui<sup>a</sup>, [fouad.erchiqui@uqat.ca](mailto:fouad.erchiqui@uqat.ca)

<sup>a</sup> Université du Québec en Abitibi-Témiscamingue

<sup>b</sup> École Polytechnique de Montréal

### Summary

Drilling can provide geological information from the subsurface at large depths. However, this information is expensive to obtain and sometimes difficult to interpret because of the lack of lateral continuity in the space between the drillings. Geophysical measurements help to increase the range of investigation around the holes up to a few hundred meters. Borehole electromagnetic methods (BEM) are particularly well suited for exploring conductive sulfide ore deposits. To improve interpretation of the BEM, a new strategy for 3D inversion of surface-borehole time domain electromagnetic (TEM) data has been developed. A quick inversion in a homogeneous half-space maps the initial guess of the exploration target. Then, using the isosurface and 3D trace envelope to delineate the anomalous conductive zone, the homogeneous space is updated to a heterogeneous initial model for the next step of the inversion. According to the test on the synthetic models, the new strategy shows better model resolution. It also allows for a faster convergence of the inversion to resolve anomalies.

### Method

#### (a) Governing equations

The surface-borehole transient electromagnetic (TEM) method uses an EM transmitter source on the surface and a receiver down in borehole. The transmitter source could be of closed-loop source or finite long wire source with impulse-voltage or AC power supply. Using the Schelkunoff potentials, the magnetic vector potential  $\mathbf{A}$  is decomposed into the primary potential (background)  $\mathbf{A}^P$  and the secondary potential  $\mathbf{A}^S$  (Nabighian, 1988; Stalnaker et al., 2006). The electric source generates  $\mathbf{A}^P$  in the half-space and  $\sigma_p$  is background conductivity. The secondary potential  $\mathbf{A}^S$  is only caused by the area where the anomalous conductivity  $\sigma_s$  is non-zero.

Using the vector theory and Lorentz gauge, the relation between the primary and the secondary vector potential in the frequency domain is defined by the Helmholtz equation as below.

$$\nabla^2 \mathbf{A}^S - i\omega\mu_0\sigma\mathbf{A}^S = i\omega\mu_0\sigma_s\mathbf{A}^P \quad (1)$$

Where  $i = \sqrt{-1}$ ,  $\sigma_s = \sigma - \sigma_p$  is the difference between the conductivity distribution ( $\sigma$ ) and the background distribution ( $\sigma_p$ ). Eq.1 is the governing equation for providing EM field modeling. The source is introduced in terms of primary EM potential that is known to the problem with background conductivity. According to the vector theory, the divergence of the curl of one vector equals to zero. The magnetic field is,

$$\mathbf{H} = \nabla \times \mathbf{A} \quad (2)$$

For the simulation of secondary potential  $\mathbf{A}^S$  in this algorithm, the edge-based finite element method is used to discretize Eq.1, the final equations system is expressed as,

$$\mathbf{K}\mathbf{A}^S = \mathbf{b} \quad (3)$$

The matrix ( $\mathbf{K}$ ) can be solved using the conjugate gradient-like (CG-like) solver with preconditioner and scaling. Then substituting the result (the secondary magnetic potential) into Eq.2, one can get the magnetic and electric fields in the frequency domain. The approximation of the numerical differentiation in Eq.2 causes an inevitable loss of accuracy. To address this issue, Raiche et al. (2003) used Green's function operators and volume integral to reduce the error in 3D numerical modeling. As the EM forward modeling is deployed in the frequency domain, the result is then converted from frequency domain to time domain by using time-frequency transformation. For the TEM forward modeling, the code Loki (Raiche et al., 2003) is used.

#### (b) Gauss-Newton inversion

For the inversion problem, the number of model cells usually is much bigger than the measured data set or survey stations. Therefore, it is an ill-posed inverse problem, which means solving an underdetermined problem. In addition, the noise contamination in data can cause non-uniqueness and instability of the inversion. To solve this problem, the general way is to improve the objective function by adding a constraining function, which is called regularization (Tikhonov, 1977; Aster et al., 2011; Menke, 1989). The Regularized Inversion Algorithm is introduced to surface-borehole EM inversion. It seeks to minimize the penalty function:

$$\Phi(\mathbf{m}) = (\mathbf{d}_{obs} - \mathbf{G}(\mathbf{m}))^T \mathbf{C}_d^{-1} (\mathbf{d}_{obs} - \mathbf{G}(\mathbf{m})) + \lambda (\mathbf{m} - \mathbf{m}_0)^T \mathbf{C}_m^{-1} (\mathbf{m} - \mathbf{m}_0) \rightarrow \min$$

$$\begin{cases} \mathbf{C}_d^{-1} = \mathbf{W}_d^T \mathbf{W}_d \\ \mathbf{C}_m^{-1} = \mathbf{W}_m^T \mathbf{W}_m \end{cases} \quad (4)$$

Where  $\mathbf{m}$  is the M-dimensional vector of the model parameters, and  $\lambda$  is the regularization parameter for controlling their contributions.  $\mathbf{W}_d$  and  $\mathbf{W}_m$  are the data and model weighting matrices (diagonal matrices), respectively. Let  $\mathbf{m}_k$  be the model parameter at the  $k^{\text{th}}$  iteration,  $\mathbf{J}$  be the sensitivity matrix obtained at  $\mathbf{m}_k$ , and  $\mathbf{r} = \mathbf{d} - \mathbf{G}(\mathbf{m}_k)$  denotes the data residual, then the iterative equation derived from the penalty function is,

$$\left[ (\mathbf{W}_d \mathbf{J})^T (\mathbf{W}_d \mathbf{J}) + \lambda \mathbf{W}_m^T \mathbf{W}_m \right] \Delta \mathbf{m} = (\mathbf{W}_d \mathbf{J})^T \cdot \mathbf{W}_d \mathbf{e} - \lambda \mathbf{W}_m^T \mathbf{W}_m (\mathbf{m} - \mathbf{m}_0) \quad (5)$$

#### (c) Isosurface and 3D trace envelope

3D TEM inversion is time-consuming and leads to a non-unique solution. To address those two challenges, one effective strategy is to set a good initial model. We propose a strategy to develop this initial model. Starting from a quick 3D inversion for field data, the initial guess ( $\mathbf{m}^{\text{pre}}$ ) contains some anomalous zones. Then, we take the averaging resistivity of the whole guess model as the resistivity of background, denoted as  $\mathbf{m}^b$ . Combining with the geological information and initial guess, using isosurface and 3D trace envelope delineate the potential anomalous zones as  $\mathbf{m}^j$  ( $j = 1, \dots, m$ );  $m$  denotes the number of anomalies. Let the domination resistivity of each anomaly be its resistivity. Therefore, the updated initial model contains two parts – background (homogeneous half-space) and potential abnormal areas.

$$\mathbf{m}_0 = \mathbf{m}^b + \sum_{j=1}^m \mathbf{m}^j \quad (6)$$

## Results and Conclusions

The synthetic model consists of two conductors of  $80 \times 80 \times 40 \text{m}$  with the resistivity of  $5 \Omega \cdot \text{m}$  and located in a half-space of  $1000 \Omega \cdot \text{m}$  (Figure 1a). The top depth is  $240 \text{m}$ . Two boreholes intersect the center of each conductor, and one borehole is located between them. The transmitter loop (Tx) of  $200 \times 200 \text{m}$  is located at  $(250 \text{m}, 200 \text{m})$  with a trapezoidal pulse as the transmitter waveform. Figure 1 illustrates the inversion results.

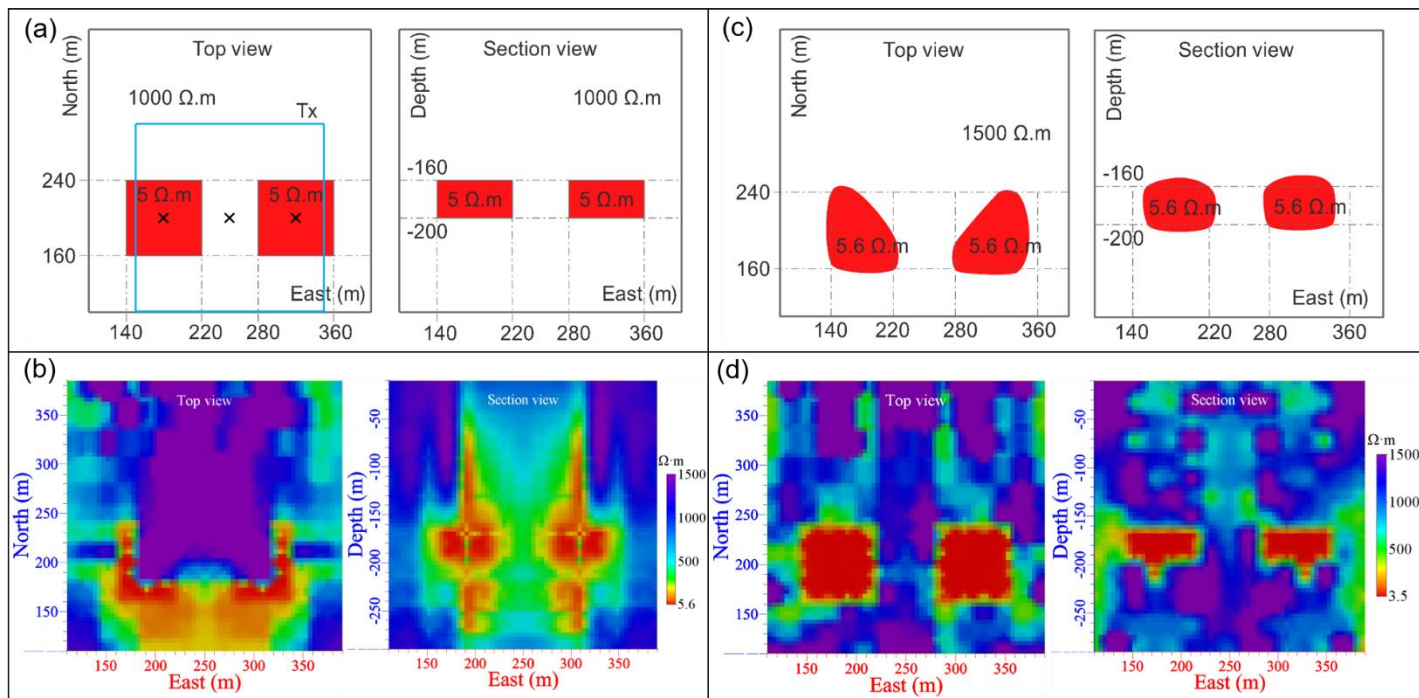


Figure 1: (a) synthetic model, (b) inversion result using half-space as initial model, (c) model delineated with isosurface and 3D trace envelope, (d) inversion result based on the updated initial model

As can be seen on Figure 1a and 1b, the conductors are not well recovered using the half-space as the initial model. Even though the horizontal locations of two conductors are right, the boundaries of the conductors are not clearly defined. After the initial model has been updated from the first inversion result, two conductors are well recovered with clear boundaries (Figure 1c and 1d).

## Acknowledgments

This work was funded by the Fonds de Recherche du Québec - Nature et technologies (FRQNT), industry partner Abitibi Geophysique and LaRonde mine of Agnico Eagle Mines Limited, Canada. The authors would like to thank the Electromagnetic Modeling Group – CSIRO Exploration & Mining for their valuable forward modeling code Loki.

## References

- Aster, R.C., Borchers, B. and Thurber, C.H., 2011. Parameter estimation and inverse problems (Vol. 90). Academic Press.
- Menke, W., 1989. Geophysical data analysis: discrete inverse theory. Academic Press.
- McGillivray, P.R., Oldenburg, D.W., Ellis, R.G. and Habashy, T.M., 1994. Calculation of sensitivities for the frequency-domain electromagnetic problem. *Geophysical Journal International*, 116(1), p.1-4.
- Nabighian, M.N., 1988. *Electromagnetic methods in applied geophysics: theory: Volume 1*, Tulsa, Oklahoma: Society of Exploration Geophysicists.
- Raiche, A., Sugeng, F., and Soininen, H., 2003. Using the Loki 3D edge-finite-element program to model EM dipole-dipole drill-hole data. *ASEG Extended Abstracts*, 2003(2), p.1-4.
- Stalnaker, J., Everett, M.E., Benavides, A. and Pierce, C.J., 2006. Mutual inductance and the effect of host conductivity on EM induction response of buried plate targets using 3-D finite element analysis, *IEEE Trans Geosci Remote Sens*, 44, p.251-259.
- Tikhonov, A.N., and Arsenin, V.I., 1977. *Solutions of ill-posed problems*. Vh Winston.
- Touma Holmberg, M., 1998. *Three-dimensional finite element computation of eddy currents in synchronous machines*. Chalmers University of Technology.